Chinese Chemical Letters 35 (2024) 109659

Contents lists available at ScienceDirect

Chinese Chemical Letters

journal homepage: www.elsevier.com/locate/cclet

# Synthesis of amine-pillar[5]arene porous adsorbent for adsorption of $CO_2$ and selectivity over $N_2$ and $CH_4$

Hui Li[a,b,c], Yanxing Qi[b,c,*], Jia Chen[a], Juanjuan Wang[a], Min Yang[b], Hongdeng Qiu[a,c,*]

[a] CAS Key Laboratory of Chemistry of Northwestern Plant Resources and Key Laboratory for Natural Medicine of Gansu Province, Lanzhou Institute of Chemical Physics, Chinese Academy of Sciences, Lanzhou 730000, China
[b] National Engineering Research Center for Fine Petrochemical Intermediates, Lanzhou Institute of Chemical Physics, Chinese Academy of Sciences, Lanzhou 730000, China
[c] University of Chinese Academy of Sciences, Beijing 100049, China

ARTICLE INFO

*Article history:*
Received 16 October 2023
Revised 23 January 2024
Accepted 13 February 2024
Available online 18 February 2024

*Keywords:*
$CO_2$ adsorption
Selective separation
Porous silica
Solid amine adsorbents
Amine-pillar[5]arene

ABSTRACT

A novel amine-modified pillar[5]arene bonded porous silica adsorbent (DETA-P5S) was designed to be applied to dynamic $CO_2$ adsorption and selective separation of $CO_2$ over $N_2$ and $CH_4$ gases mixture. The results demonstrated that reasonable introduction of DETA into the BE-P5 bonded silica support has significantly increased the adsorption capacity of $CO_2$. The DETA-P5S has the optimal adsorption capacity of 9.1 mmol/g with 5 vol% $CO_2$ at 40 °C. The main reason of this increased capacity could be attributed to the enhanced $CO_2$ diffusion into porous adsorbent for its better dispersion in the pores of amine-pillar[5]arene cavity and active site of DETA. Furthermore, the dynamic saturation adsorption capacities of DETA-P5S were 7.11 (0.37) and 6.18 (0.44) mmol/g for $CO_2/N_2$ and $CO_2/CH_4$, respectively, both the gas mixtures showed high separation selectivity. Simultaneously, the DETA-P5S can maintain outstanding $CO_2$ adsorption capacity after fifteen regeneration cycles. Consequently, the designed DETA-P5S could serve as a promising adsorbent for $CO_2$ capture and storage.



Excessive emissions of carbon dioxide ($CO_2$), stemming from the combustion of fossil fuels, are deemed major contributors to the greenhouse effect [1–3]. To the best of our understanding, $CO_2$ also serves as a valuable resource the production of fine chemicals, beverage additives, and other fields [4,5]. Recent studies have confirmed that $CO_2$ capture and storage (CCS) would be a potential method for carbon reduction [6]. A myriad of capture adsorption techniques and materials have been studied to $CO_2$ capture [7–9]. Thereinto, solid adsorbent was believed to be the most potential one with considerations to their simple preparation, good repeatability and stability [10]. However, these adsorbents have shortcomings of poor selectivity or low adsorption capacity. Therefore, there is a pressing need to develop novel solid adsorbents that enhance $CO_2$ capture efficiency.

To investigate the practical separation efficacy of adsorbents, there is a significant emphasis on enhancing the $CO_2$ capacity with selectivity for $CO_2$ over $N_2$ and $CH_4$. Additionally, factors such as stability and regenerability are crucial in adsorbent development [11,12]. Recently, solid amine adsorbents obtained by grafting or impregnating porous silica with organic amines, have garnered attention due to their superior physical and chemical properties, which are notably characterized by high selectivity, easy regeneration and potential prospects of $CO_2$ capture [13–16]. This has the potential to significantly enhance the adsorption process compared to raw porous materials. The adsorption capacity of $CO_2$ and selectivity of porous solid amine adsorbents may be contingent upon factors such as specific surface area, pore volume, porosity, and the interaction between gas molecules and active sites within the main skeleton groups. Notably, pore volume and active sites are crucial for the adsorption capacity, particularly in the context of selective adsorption [17,18]. However, how to optimize the design scheme for high adsorption capacity along with its selectivity is still a great challenge [19]. In the separation of $CO_2$ from $N_2$ and $CH_4$, the similarity in molecular sizes and intermolecular interactions plays a significant role [20]. All previously reported studies have clearly indicated that the strategic introduction of low-density molecules and organic amines into porous adsorbents may serve as a feasible method for synthesizing materials with high $CO_2$ adsorption capacity. Additionally, these materials can selectively separate $CO_2/N_2$ and $CO_2/CH_4$ gases [21–23].

Herein, in view of previous studies on pillar[5]arenes [24–27], we reported a novel amine-pillar[5]arene based solid

* Corresponding authors.
*E-mail addresses:* qiyx@licp.cas.cn (Y. Qi), hdqiu@licp.cas.cn (H. Qiu).

https://doi.org/10.1016/j.cclet.2024.109659
1001-8417/

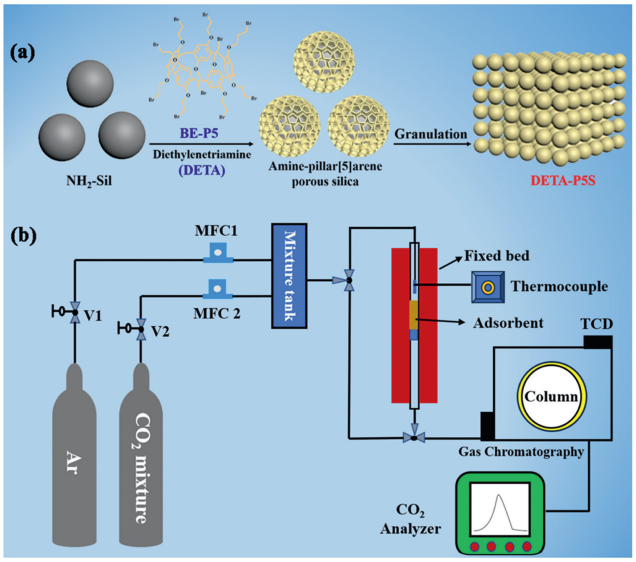


**Fig. 1.** (a) Synthesis of DETA-P5S. (b) Schematic diagram of fixed-bed (FD-2000) reactor for $CO_2$ capture.

amine adsorbent, named DETA-P5S, which constructed from bromo–pillar[5]arene (BE-P5), diethylenetriamine (DETA) and porous silica as shown in Fig. 1a and Fig. S1 (Supporting information). Subsequently, the adsorption process of $CO_2$ and selectivity separation for $CO_2$ over $N_2$ and $CH_4$ on DETA-P5S were performed on a fixed-bed (Fig. 1b). The physicochemical properties of adsorbents were systematically studied by FT-IR, scanning electron microscopy (SEM), thermogravimetric analysis (TGA), BET, XPS, MIP, *etc*. The effects of gas flow rate, amount, adsorption temperature, and adsorption mechanism on $CO_2$ adsorption process were also investigated.

In FT-IR spectra, a broad band at 3550~3300 $cm^{-1}$ was referred to the stretching vibration of N–H and Si–OH. The peaks at 2933 and 2856 $cm^{-1}$ were assigned to symmetric and asymmetric stretching vibration corresponding to C–H bonds, respectively. The peak at 1634 $cm^{-1}$ was identified as the stretching vibration of C=C on benzene ring, which indicated the successful introduction of BE-P5. Additionally, peaks at 1506 and 1240 $cm^{-1}$ were attributed to the N–H deformation vibration of aliphatic secondary amines and C–N stretching vibration, respectively, which confirmed the successful modification of DETA. The peaks at 1095, 807 and 466 $cm^{-1}$ were characteristic vibrational peaks of Si–O–Si bonds. These data confirmed the successful preparation of DETA-P5S (Fig. 2a). SEM exhibited agglomerating morphology of silica particles with rough surface and apparent silica pore (Fig. 2b). Transmission electron microscopy (TEM) investigation revealed that there was significant pore structure of silica particle stacking in DETA-P5S (Fig. S4 in Supporting information). TGA curves of $NH_2$-Sil, BE-P5S, and DETA-P5S under $N_2$ flow were examined and presented in Fig. 2c. The findings indicated that pristine $NH_2$-Sil has high thermal stability in a protective atmosphere, the weight loss was only 6.62% even after being heated to 750 °C. The DETA-P5S also exhibited excellent thermal stability until the temperature reached 260 °C, a more rapid decrease stage for the quality of BE-P5S and DETA-P5S was appeared in the temperature range of 260–750 °C. This could be attributed to the decomposition, combustion and volatilization of BE-P5 or DETA within the adsorbents. Ultimately, the loss rate of BE-P5S and DETA-P5S were 11.69% and 15.54%, which indicated that the bonding amount of BE-P5 and DETA were reached 5.07% and 3.85%, respectively. The $N_2$ adsorption-desorption isotherms and BJH pore size distribution curves of DETA-P5S was shown in Fig. 2d, it can be found that DETA-P5S has a typical IV type of $N_2$ desorption curves with a large surface area of 231.65 $m^2/g$, which

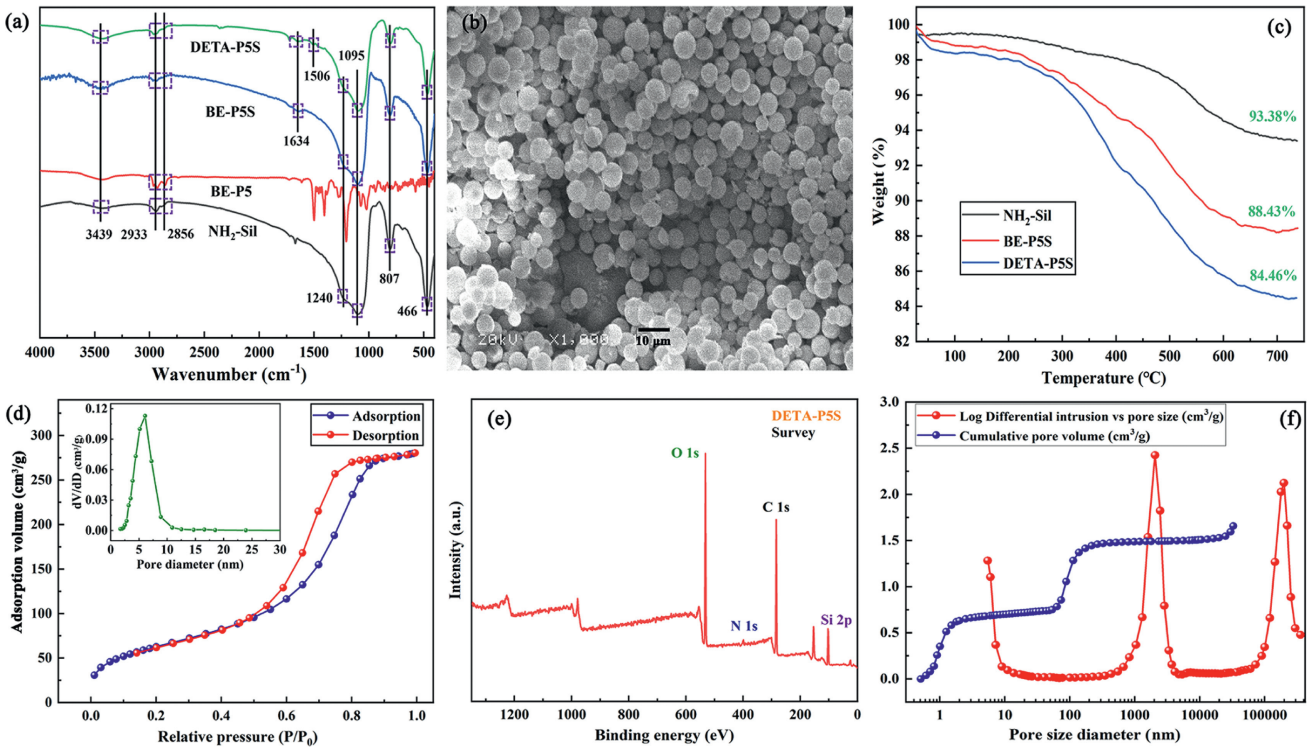


**Fig. 2.** Characterization of adsorbents: (a) FT-IR spectra of $NH_2$-Sil, BE-P5, BE-P5S, and DETA-P5S, (b) SEM of DETA-P5S, (c) TG of $NH_2$-Sil, BE-P5S, and DETA-P5S, (d) $N_2$ adsorption/desorption isotherms of DETA-P5S, (e) XPS of DETA-P5S, (f) MIA of DETA-P5S.

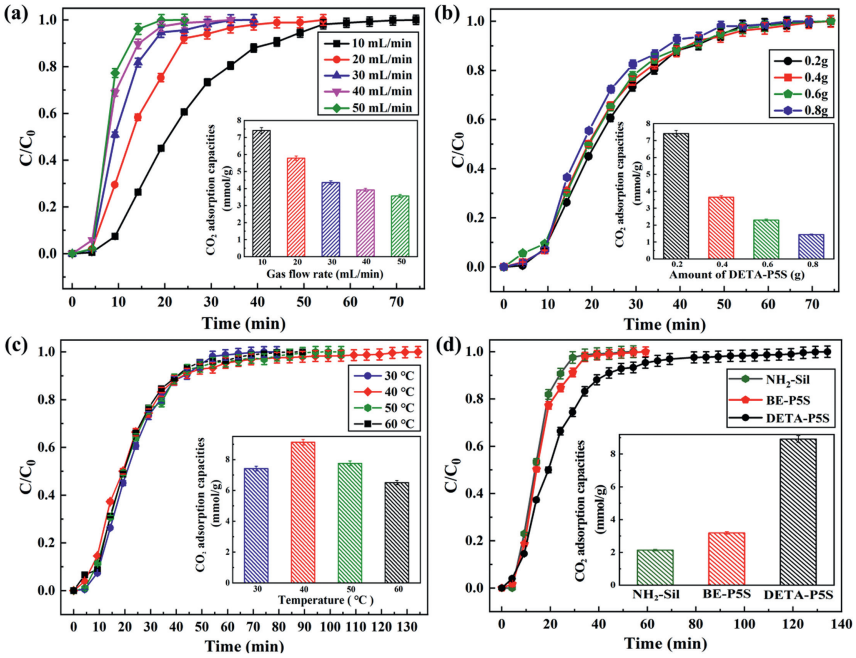


**Fig. 3.** (a) Effect of gas flow rate for $CO_2$ adsorption capacity of DETA-P5S. (b) Effect of DETA-P5S amount for $CO_2$ adsorption capacity. (c) Effect of adsorption temperature for $CO_2$ adsorption capacity. (d) $CO_2$ adsorption capacity of different adsorbents.

indicated DETA-P5S has mesoporous pore structure. In addition, X-ray photoelectron spectroscopy (XPS) confirmed the presence of C, N, O, and Si elements (Fig. 2e). Elemental analysis (EA) also showed that the content of DETA-P5S for N, C, H reached 2.68%, 13.28% and 1.63% (Table S1 in Supporting information), confirmed the successful grafting of DETA on BE-P5S. Moreover, energy-dispersive X-ray spectroscopy (EDS) analysis in SEM shows that O, C, and N elements were uniformly distributed over DETA-P5S (Fig. S5 in Supporting information). Mercury intrusion porosimetry revealed that the total pore volume of DETA-P5S was 1.66 $cm^3/g$, with a pore size was 77.17 nm. The porosity reached 67.73%, which provided favorable conditions for the adsorption of $CO_2$ (Fig. 2f). While large pores formed may be the pores between porous silica in aggregate granulation, and the mesoporous pores originate from the porous silica.

The evaluation of $CO_2$ adsorption process was conducted using a fixed-bed (FD-2000) reactor, equipped with a 6 mm diameter quartz reaction tube. The saturation adsorption capacity of $CO_2$ was determined by utilizing the breakthrough curve according to Zhao *et al.* [28]. The adsorbent was first treated for 50 min at 120 °C with a flow rate of 20 mL/min Ar to remove pre-adsorbed residual solvents, then adjusted to corresponding adsorption conditions and carried out $CO_2$ adsorption process. An adsorption cycle was considered complete when the outlet $CO_2$ concentration matched the inlet concentration. Subsequently, Ar was purged again to desorption at 120 °C for 50 min, then proceed to the next $CO_2$ adsorption at corresponding requirements. Throughout the experiment, the $CO_2$ concentration of the reactor outlet was measured using gas chromatography, coupled with a TCD detector.

In order to investigate the optimal adsorption capacity of DETA-P5S for $CO_2$, the breakthrough curves were measured at different factors like flow rates, amount of adsorbent, adsorption temperatures, and different adsorbents. The effect of flow rate on the breakthrough curve of DETA-P5S was operated as Fig. 3a. It was found that the $CO_2$ saturation adsorption capacity for $CO_2$ reached 7.4 mmol/g when 0.2 g of DETA-P5S at a flow rate of 10 mL/min. However, both the breakthrough time and saturation adsorption capacity for $CO_2$ declined as the gas flow rate increased. It may be that working at a faster gas flow rate reduced the retention time of $CO_2$ gas in the fixed bed, thus resulted in a decrease of adsorption, eventually leaded to earlier breakthrough times, these characteristics are consistent with the reports [29].

Subsequently, the effect of DETA-P5S amount for $CO_2$ adsorption capacity was investigated with flow rate of 10 mL/min at 30 °C (Fig. 3b), and the breakthrough time was shortened and the $CO_2$ saturated adsorption capacity decreased with the increase of DETA-P5S increased from 0.2 g to 0.8 g. Based on the basis of adsorption mechanism, the adsorption capacity of acid gas may depend on the amine proportion in DETA-P5S. It could be concluded that a certain amount of DETA-P5S could enhance $CO_2$ adsorption capacity for dominant adsorption mode. However, when too much adsorbent was packed, the column height of the adsorbent increased, and the diffusion resistance of $CO_2$ through the adsorbent pores was increased accordingly, which reduced the contact time between $CO_2$ and the active amine of the internal adsorbent. As a result, the saturation adsorption capacity was reduced. Therefore, the saturation adsorption capacity of $CO_2$ is related to the amount of DETA-P5S in specific reaction tubes.

Temperature significantly influences the $CO_2$ adsorption capacity, Fig. 3c represented the effect of adsorption temperature on $CO_2$ adsorption capacity from 30 °C to 60 °C on 0.2 g DETA-P5S at a 10 mL/min flow rate. the results revealed that the $CO_2$ saturation adsorption capacity of DETA-P5S reached 9.1 mmol/g when the temperature at 40 °C, however, further temperature increases lead to a decrease in adsorption capacity, these results indicated that the adsorption of $CO_2$ to EDTA-P5S may be a kinetics-controlled process. When increased the temperature, the diffusion resistance of $CO_2$ decreases, the structure of alkyl chain in DETA-P5S stretched and exposed more active site, which leads to a significant increase in $CO_2$ capture capacity. However, with the further increased of temperature, the desorption of $CO_2$ from the adsorption site in the pore may become more priority, resulting in the reduction of $CO_2$ adsorption capacity. Therefore, DETA-P5S at 40 °C was an important factor as a candidate material for $CO_2$ adsorption.

Furthermore, with multiple modification in synthesis process, the $CO_2$ adsorption capacity may be different. To examine the impact of DETA derivatives on adsorption capacity, we investigated

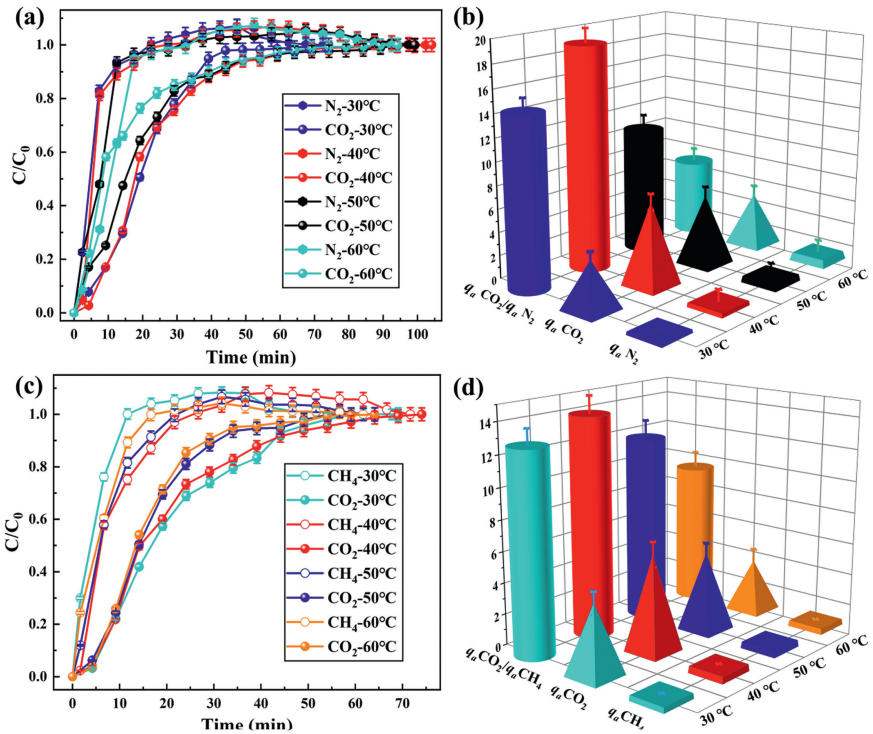


**Fig. 4.** (a) Effect of temperature on selectivity of $CO_2/N_2$ for DETA-P5S. (b) Saturated adsorption capacity and selectivity of $CO_2/N_2$. (c) Effect of temperature on selectivity of $CO_2/CH_4$ for DETA-P5S. (d) Saturated adsorption capacity and selectivity factor of $CO_2/CH_4$.

the $CO_2$ adsorption capacity of control adsorbents $NH_2$-Sil and BE-P5S (Fig. 3d). The saturated adsorption capacity of $CO_2$ on DETA-P5S was found to be the highest when compared to the other two adsorbents. The results indicated that the introduction of DETA on pillar[5]arene bonded porous silica greatly enhanced the adsorption capacity of $CO_2$. Considering the great change of $CO_2$ adsorption capacity after the introduction of DETA and BE-P5, this method can provide a new strategy for the development of $CO_2$ solid amine adsorbent.

To further assess the practical separation performance of DETA-P5S, the effect of temperature on dynamic adsorption performance selectivities of DETA-P5S for $CO_2/N_2$ and $CO_2/CH_4$ were evaluated through breakthrough tests, respectively. The two ternary gas mixtures $CO_2/N_2/Ar$ and $CO_2/CH_4/Ar$ with a composition of 5/5/90 were used at a flow rate of 10 mL/min at 30∼60 °C. The adsorption time of $CO_2$ in whole adsorption process was longer than that of $N_2$ and $CH_4$, indicated that the adsorption capacity of $CO_2$ was strong, and the breakthrough time was longer than that of $N_2$ and $CH_4$. The breakthrough curve clearly shown that DETA-P5S has good separation potential for $CO_2$ over $N_2$ and $CH_4$. The dynamic saturation adsorption capacities of DETA-P5S were 7.11 (0.37) and 6.18 (0.44) mmol/g for $CO_2/N_2$ (Figs. 4a and b) and $CO_2/CH_4$ (Figs. 4c and d), respectively, both the gas mixtures showed high separation selectivity. These results have demonstrated that DETA-P5S is a promising absorbent for the adsorption of $CO_2$ in preference to $CH_4$ and $N_2$.

As an excellent adsorbent, in addition to high absorption capacity and selective separation, there are advantages of stability at cyclic adsorption. During operation, the adsorption temperature of 40 °C and desorption temperature of 110 °C were performed for DETA-P5S in $CO_2$ cyclic adsorption capacity (Fig. 5a), the study concluded that the adsorption capacity of $CO_2$ diminished from 8.4 mmol/g to 7.6 mmol/g following 15 cycles of adsorption and desorption, yet it still retained an exceptionally high $CO_2$ adsorption capacity. The findings suggested that DETA-P5S could be effectively utilized in cyclic $CO_2$ adsorption operations.

*In situ* infrared spectroscopy was employed to study the adsorption mechanism of $CO_2$ on DETA-P5S. As shown in Fig. 5b and Fig. S6 (Supporting information), the intensity of stretching vibration at 3728∼3533 $cm^{-1}$ was confirmed to be due to the binding effect between $CO_2$ and –OH on silicas. The peak at 3345 $cm^{-1}$ was the asymmetric stretching vibration peak of $NH_2$, and the peak at 3231 $cm^{-1}$ was the symmetric stretching vibration peak of $NH_2$ and NH. Peak at 3105 $cm^{-1}$ was the stretching vibration of N–H. The intensity of stretching vibration at 2381 $cm^{-1}$ and 2290 $cm^{-1}$ were thought to be stretching vibration of $CO_2$, the peak at 2170 $cm^{-1}$ was the vibration peak of $NH_2^+$–$COO^-$. Peaks at 1711 $cm^{-1}$ was vibration adsorption peaks of C=O bond in –NCOOH. Peak at 1697 $cm^{-1}$ is the deformation vibration peak of $NH_3^+$. Peaks at 1557∼1553 $cm^{-1}$ were the stretching vibration peak of $COO^-$. Peak at 1516 $cm^{-1}$ was the stretching vibration peak of C–N, and peaks at 651 $cm^{-1}$ was assigned for $CO_2$ deformation vibration. The adsorption peaks of $NH_3^+$ and $NH_2^+$ gradually intensified mainly because $CO_2$ reacted with $NH_2$ and NH. This was consistent with dynamic $CO_2$ adsorption mechanism of solid amine adsorbent [30–32]. Consequently, the $CO_2$ adsorption of adsorbent follows anionic and cationic mechanisms on DETA-P5S, finally forming ammonium ions and carbamate.

Solid-state $^{13}C$ MAS NMR spectrum was further conducted to investigate the adsorption mechanism for whether there was a formation of carbamate (Fig. 5c), the distinct resonance at 168 ppm indicated the formation of carbamate after adsorbed $CO_2$ by DETA-P5S. Therefore, DETA-P5S has the ability to selectively adsorption of $CO_2$, as well as the amide and hydroxyl group in its framework have a synergistic effect, they play an important role in the interaction with $CO_2$ in both chemisorption and physisorption (Fig. 5d). Lastly, the *pseudo*-first-order model, *pseudo*-second-order model and Avrami kinetic model were fitted to the adsorption

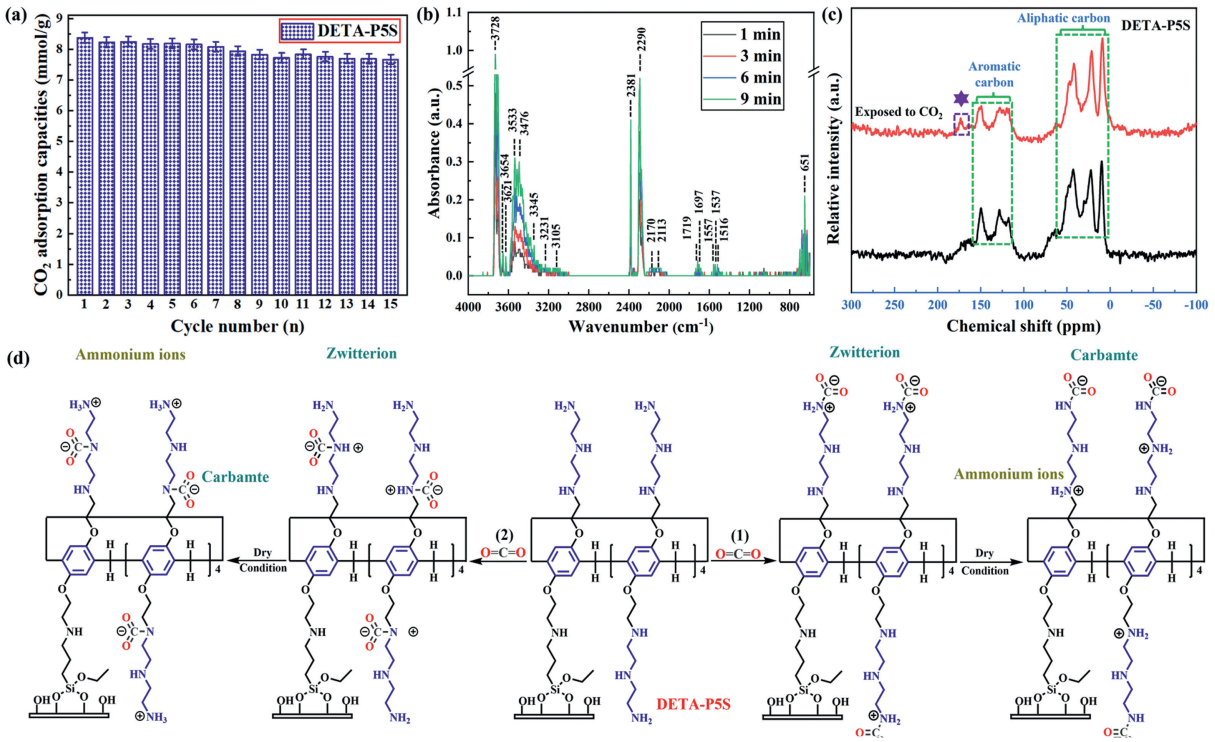


**Fig. 5.** (a) The cyclic $CO_2$ adsorption of DETA-P5S. (b) Two-dimensional *in situ* IR spectrum of DETA-P5S. (c) Solid-state $^{13}C$ MAS NMR spectrum of DETA-P5S. (d) Reaction mechanism for DETA-P5S with $CO_2$.

process, the results suggested that the Avrami model can accurately predict the adsorption kinetics of DETA-P5S, the correlation coefficient of $R^2$ was above 0.9977 and the adsorption process has both physical and chemical adsorption, but physical adsorption plays a dominant role in the adsorption process (Fig. S7 and Table S2 in Supporting information) [7].

In conclusion, a novel amine-pillar[5]arene functionalized $CO_2$ porous adsorbents (DETA-P5S) with high $CO_2$ adsorption capacity was prepared for selective separation $CO_2$ over $N_2$ and $CH_4$. The DETA-P5S preferentially adsorbs $CO_2$ over $N_2$ and $CH_4$ for its primary and secondary amine with a weakly nucleophilic property, which were able to interact with $CO_2$. The effects of gas flow rate, amount of adsorbent, and adsorption temperature on $CO_2$ adsorption capacities were systematic studied. The DETA-P5S has the optimal capture amount of 9.1 mmol/g with 5 vol% $CO_2$ flow rates at 40 °C, which indicated that the introduction of DETA provided amino active sites, while the cavity of pillar[5]arene provided capture pores, thereby promoting $CO_2$ adsorption. Moreover, the dynamic saturation adsorption capacities of DETA-P5S were 7.11 (0.37) and 6.18 (0.44) mmol/g for $CO_2/N_2$ and $CO_2/CH_4$, respectively, both the gas mixtures showed high separation selectivity. Simultaneously, the DETA-P5S also maintained an outstanding $CO_2$ adsorption capacity even after ten regeneration cycles. *In-situ* FTIR and solid-state $^{13}C$ MAS NMR spectrum confirmed that the $CO_2$ adsorption process on DETA-P5S was consistent with zwitterionic mechanism. This study demonstrates that amine-pillar[5]arene solid porous adsorbent with organic amine modification and could provide a facile protocol for the challenging $CO_2$ capture.

## Declaration of competing interest

The authors declare that they have no known competing financial interests or personal relationships that could have appeared to influence the work reported in this paper.

## Acknowledgments

The authors are thankful for financial supports from National Natural Science Foundation of China (No. 22204169), Gansu Natural Science Foundation (Nos. 23JRRA619, 21JR7RA076) and Scientific and Technological Program of Chengguan District, Lanzhou (No. 2023JSCX0037).

## Supplementary materials

Supplementary material associated with this article can be found, in the online version, at doi:10.1016/j.cclet.2024.109659.

## References

[1] L. Zhang, S.H. Lin, Y.P. Liu, et al., Inorg. Chem. 62 (2023) 8058–8063.
[2] M.M. Abdelnaby, N.A.A. Qasem, B.A. Al-Maythalony, et al., ACS Sustain. Chem. Eng. 7 (2019) 13941–13948.
[3] M. Breunig, M. Dorner, J. Senker, J. Mater. Chem. A 9 (2021) 12797–12806.
[4] L. Li, N. Zhao, W. Wei, et al., Fuel 108 (2013) 112–130.
[5] S. Ravi, J. Kim, Y. Choi, ACS Sustain. Chem. Eng. 11 (2023) 1190–1199.
[6] J.J. Dai, D.Y. Xie, Y. Liu, et al., Ind. Eng. Chem. Res. 59 (2020) 7866–7874.
[7] G.J. Zhang, P.Y. Zhao, L.X. Hao, et al., Sep. Purif. Technol. 209 (2019) 516–527.
[8] M.M. Zhang, L. Chen, Z.Y. Yuan, et al., Ind. Eng. Chem. Res. 62 (2023) 8902–8910.
[9] E. Jeon, S.Y. Moon, J.S. Bae, et al., Angew. Chem. Int. Ed. 55 (2016) 1318–1323.
[10] G.J. Zhang, P.Y. Zhao, L.X. Hao, et al., J. $CO_2$ Util. 24 (2018) 22–33.
[11] A.M. Varghese, G.N. Karanikolos, Int. J. Greenh. Gas Control. 96 (2020) 103005.
[12] L.J. Wei, W. Wei, N. Xue, et al., ACS Appl. Mater. Interfaces 13 (2021) 5814–5822.
[13] K.S.K. Reddy, A.M. Varghese, A.E. Ogungbenro, et al., ACS Appl. Eng. Mater. 1 (2023) 720–733.
[14] Y. Le, D. Guo, B. Cheng, et al., J. Colloid Interface Sci. 408 (2013) 173–180.
[15] G.J. Zhang, P.Y. Zhao, Y. Xu, J. Ind. Eng. Chem. 54 (2017) 59–68.
[16] G.J. Zhang, P.Y. Zhao, Y. Xu, et al., ACS Appl. Mater. Interfaces 10 (2018) 34340–34354.
[17] J. Lu, J. Zhang, J. Mater. Chem. A 2 (2014) 13831–13834.
[18] B. Zhang, G.Y. Li, J. Yan, et al., J. Phys. Chem. C 119 (2015) 13080–13087.
[19] S. Bali, J. Leisen, G.S. Foo, et al., ChemSusChem 7 (2014) 3145–3156.
[20] D.V. Quang, A. Dindi, M.R.M. Abu-Zahra, ACS Sustain. Chem. Eng. 5 (2017) 3170–3178.
[21] J. Peng, Z. Liu, Y. Wu, et al., ACS Appl. Mater. Interfaces 14 (2022) 21089–21097.

[22] K.K. Wang, H.L. Huang, D.H. Liu, et al., Environ. Sci. Technol. 50 (2016) 4869–4876.
[23] M. Babaei, S. Salehi, M. Anbia, et al., J. Chem. Eng. Data 63 (2018) 1657–1662.
[24] H. Li, Y.R. Zhu, B.B. Shi, et al., Chin. J. Chem. 33 (2015) 373–378.
[25] H. Li, K.J. Quan, X. Yang, et al., Trends Anal. Chem. 131 (2020) 116026.
[26] H. Li, X.P. Wang, C.X. Shi, et al., Chin. Chem. Lett. 34 (2023) 107606.
[27] C.X. Shi, H. Li, X.F. Shi, et al., Chin. Chem. Lett. 33 (2022) 3613–3622.
[28] P.Y. Zhao, G.J. Zhang, Y. Xua, J. $CO_2$ Util. 34 (2019) 543–557.
[29] R. Sabouni, H. Kazemian, S. Rohani, Environ. Sci. Technol. 47 (2013) 9372–9380.
[30] Y. Zhai, S.S.C. Chuang, Energy Technol. 53 (2017) 510–519.
[31] P.Y. Zhao, G.J. Zhang, Y. Xu, et al., Energy Fuels 33 (2019) 3357–3369.
[32] G.S. Foo, J.J. Lee, C.H. Chen, et al., ChemSusChem 10 (2017) 266–276.